Signature: © Pol J Radiol, 2015; 80: 515-522
DOI: 10.12659/PJR.894250

Polish Journal of Radiology
www.PolRadiol.com
ORIGINAL ARTICLE

Received: 2015.03.27
Accepted: 2015.06.29
Published: 2015.11.25

Efficiencies of Some Spherical Ion Chambers in Continuous and Pulsed Radiation: A Numerical Evaluation

Authors' Contribution:
A Study Design
B Data Collection
C Statistical Analysis
D Data Interpretation
E Manuscript Preparation
F Literature Search
G Funds Collection

Ahmed M. Maghraby[1,2] ABCDEF

[1] Department of Physics, Faculty of Science – Alzulfi – Almajmaah University, Almajmaah, Saudi Arabia
[2] Department of Radiation Dosimetry, National Institute of Standards (NIS), Ionizing Radiation Metrology Laboratory, Giza, Egypt

Author's address: Ahmed M. Maghraby, National Institute of Standards (NIS), Ionizing Radiation Metrology Laboratory, Tersa st. 12211, Giza, P.O. Box: 136, Egypt, e-mail: maghrabism@yahoo.com

Summary

Background: Evaluation of the collection efficiencies of ion chambers is a necessity for the proper evaluation of radiation quantities in different applications. Overall collection efficiency is the product of three different values: collection efficiencies considering contributions of, volume recombination, back-diffusion loss and initial recombination, the later may be neglected at low charge rates.

Material/Methods: Five common spherical ion chambers of different volumes and specifications were included in this study for the evaluation of volume recombination collection efficiency and back diffusion collection efficiency for continuous and pulsed radiation and at different values of the applied polarizing potential. Through current work there is an attempt of focusing on how the selection of ion chamber dimensions may affect the overall collection efficiency in addition to the proper selection of other influencing parameters.

Results: Collection efficiencies considering volume recombination (*fv*) for five spherical ion chambers of common types were evaluated for continuous and pulsed radiation over a wide range of polarizing potential. The relation between the ion chamber volume and its evaluated collection efficiencies were studied for both continuous and pulsed radiation; transit time values for the ion chambers included in this study were evaluated at different values of applied potential. Also, collection efficiencies considering diffusion current values (*fd*) were evaluated for the five chambers, and plotted versus the applied polarizing potential.

Conclusions: Through this study it was feasible to evaluate numerically the collection efficiencies of some spherical ion chambers considering volume recombination and back diffusion effects; the affecting parameters were studied and highlighted.

MeSH Keywords: Air Ionization • Efficiency • V(D)J Recombination

PDF file: http://www.polradiol.com/abstract/index/idArt/894250

Background

The importance of ion chamber efficiency evaluation as a basic step in the determination of radiation doses in medical radiation applications is reflected by the accuracy requirements recommended for the delivery of tumor dose as the final step where it was recommended that ±5% should be the maximum uncertainty associated to this process [1]. This value of maximum uncertainty associated to the delivery of tumor dose includes all factors associated or related to this process such as uncertainty in basic dosimetry, patient positioning, and errors in clinical settings [2].

In basic dosimetry, the aim is to evaluate experimentally some radiation quantity according to well-recognized procedures and using associated formulations and recommended equipment and tools. This is usually achieved via dosimetry protocols [3–7]. The most common dosimetry

Table 1. Dimensional characteristics of spherical chambers included in the current study and the recommended polarizing potential.

Ion chamber type	Volume cm^3	a (mm)	b (mm)	Recommended potential (V)
A3 Exradin	3.6	9.55	1.05	300–1000
A4 Exradin	30.0	19.05	2.05	500–1000
A5 Exradin	100	28.60	3.25	800–1000
A6 Exradin	800	57.20	5.80	1000
A8 Exradin	15700	155.60	11.20	1000

systems used worldwide in basic dosimetry for all medical applications are the ion chambers [8].

When incident radiation interacts with the ion chamber walls, buildup cap, sleeve, or phantom through photoelectric effect, Compton scattering and pair production (according to conditions of interactions, it usually results in the production of energetic electrons; when these electrons enter the sensitive volume of the ion chamber, they ionize air inside the sensitive volume of the chamber which results in the production of positive ions and low energy electrons. The later can be attached easily by oxygen molecules forming negative ions [2].

Ideally, all charges produced within the volume of the ion chamber are collected by the corresponding electrode. However, some factors lead to the lack of complete collection of these charges [9]. These factors are related to different origins either connected with the geometrical structure of the ion chamber, applied voltage, or the beam type and strength [10,11].

Cavity ion chambers are of two types, either parallel-plate ion chambers usually used for the superficial x-rays, low energy electrons, and for surface doses evaluation, or the thimble type chambers usually used in photon or electron beams above 10 MeV.

In the current work, collection efficiencies of some spherical ion chambers are evaluated numerically in order to find out differences among types or models in general, although it still necessary to evaluate experimentally some related correction factors for each individual ion chamber within the same type. It is important to note that this work is just an academic study and hence it was not restricted to those values of the applied potential recommended by the manufacturer in calculations. The dimensional characteristics of spherical chambers included in the current study are included in Table 1, and air was assumed to be the filling gas.

Material and Methods

Away from the ideal saturation current in an ionization chamber (I_s), real output current (I) is usually lower due to incomplete charge collection as a result of several effects, being: Initial recombination, Back-diffusion to electrodes, and Volume recombination [12]. The collection efficiency for an ion chamber (*f*) can be evaluated according to the following relation:

$$f = f_i f_v f_d \quad (1)$$

where *fi*, *fv,* and *fd* are collection efficiencies considering contributions of initial recombination, volume recombination, and back-diffusion loss, respectively [13]. Initial recombination (also called columnar recombination) does not depend on the radiation dose or dose rate. This process occurs when the positive and negative ions formed in the same charged-particle track meet and recombine. For initial recombination, the number of tracks formed within the chamber is not important and hence this effect is dose-rate-independent. In contrast, volume recombination (also called general recombination) takes into account recombination of ions formed from different origins (different tracks) and hence the number of tracks formed within the chamber affects the value of the general recombination and hence it is dependent on the radiation dose rate [14,15], the total recombination is the sum of these two effects. Additionally, loss of ions due to diffusion is independent on the radiation dose rate and considers the back diffusion of positive and negative ions to an anode and cathode respectively [16].

Initial recombination is most probable in high ion density tracks like those formed by alpha particles or other high LET radiation, like energetic electrons passing through high-pressure gases while it is negligible in usual clinical uses and other cases.

So, for the recombination process we will consider only volume recombination in the current study. For continuous radiation, and according to the Boag's theory [17], the collection efficiency *fv* can be obtained from the following formula:

$$f_v = 1 - \eta^2 \quad (1),$$

where $$\eta^2 = \frac{(M^2/6).d^4.\dot{q}}{V^2} \quad (2),$$

and *d* is an effective electrode spacing, *M* is an empirical constant depending on the nature of the gas ($1.99\times10^7\pm1.7\%$ $Vm^{1/2}s^{1/2}C^{-1/2}$ for air), $\dot{q}$ is the rate of charge collected per unit volume of the gas ($cm^{-3}s^{-1}$), and *V* is the polarizing potential [18].

In case of pulsed radiation, *fv* can be calculated using the following formula:

$$f_v = \frac{\nu}{\exp(\nu) - 1} \quad (3),$$

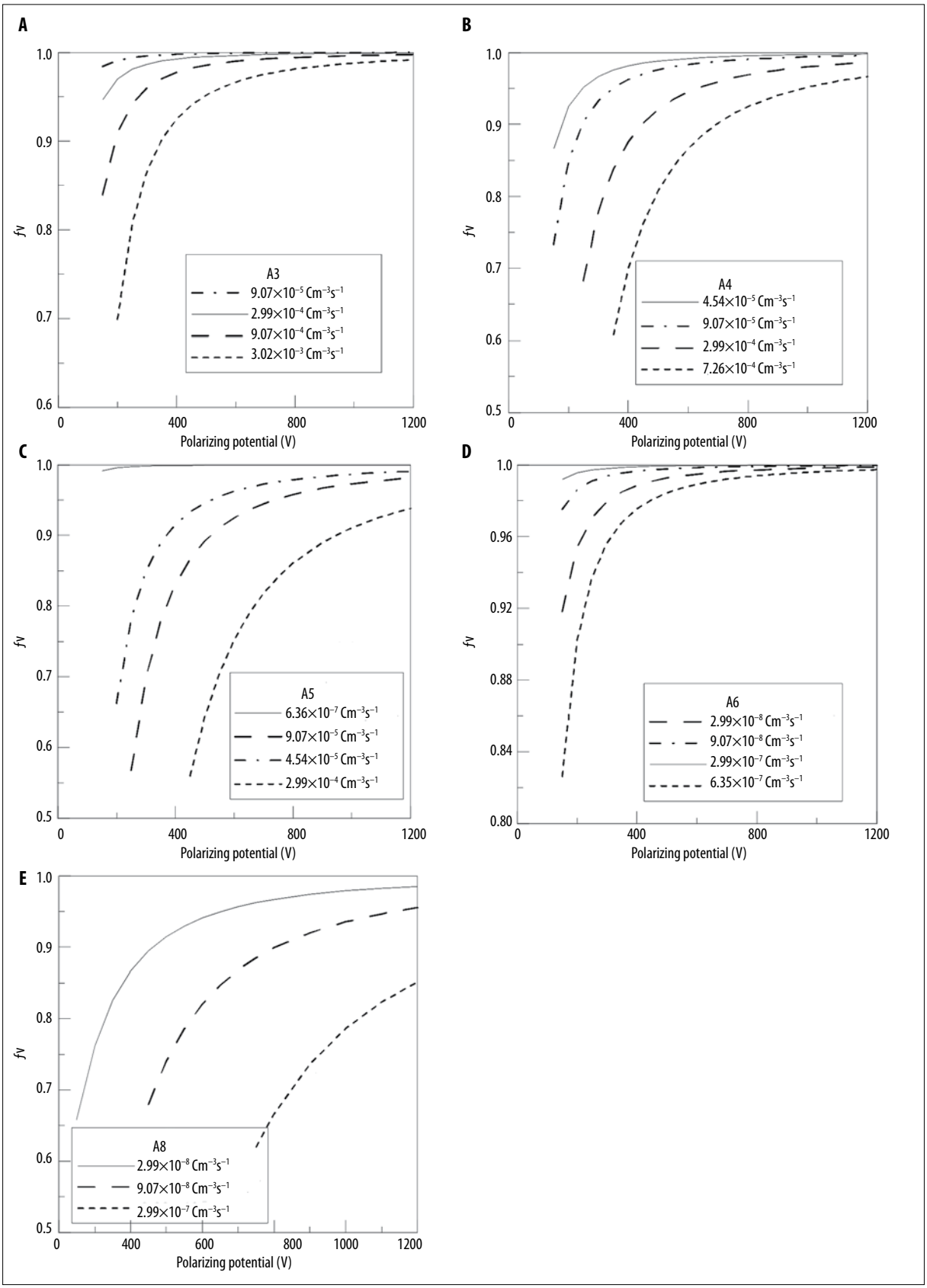

Figure 1. Evaluated collection efficiencies in continuous radiation for different ion chambers as a function in the applied polarizing potential in an ascending order with respect to the chamber volume, values evaluated at different values of charge rate per unit volume ($\dot{q}$): (**A**) A3-Exradin, (**B**) A4-Exradin, (**C**) A5-Exradin, (**D**) A6-Exradin, (**E**) A8-Exradin.

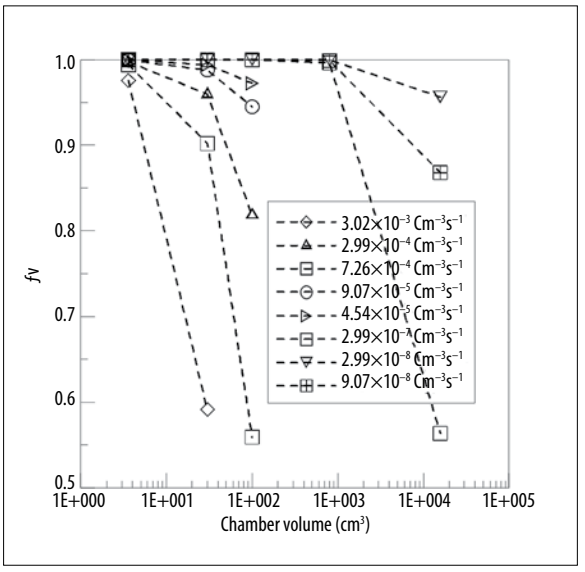

Figure 2. Volume collection efficiency for continuous radiation (f_V) values corresponding to different values of chamber volume (cm^3) evaluated at different charge rate values ($\dot{q}$).

where $\nu = \frac{\mu . d^2 q}{V}$ (4),

$$\mu = \frac{\alpha / e}{k_1 + k_2} \quad (5)$$

where q is the initial charge density per pulse of the positive and negative ions collected by the ion chamber during irradiation, α is the ion recombination coefficient, e is the charge of an electron, k_1 is the mobility of positive ions, k_2 is the mobility of the negative ions, and μ depends on the lifetime of ions in the chamber and for air it equals to 3.02×10^{10} $mC^{-1}V$ [19].

The effective electrode spacing for the spherical chambers (d) can be calculated using the following formula [17–20]:

$$d = \frac{(a-b)}{\sqrt{3}} . [\frac{a}{b} + 1 + \frac{b}{a}]^{\frac{1}{2}} \quad (6)$$

Where 'a' is the internal radius of the outer electrode and 'b' is the external radius of the inner electrode.

For the decrease in output current due to back diffusion in spherical chambers, an approximate solution was presented by Takata, N. et al. [21]:

$$\frac{\delta I}{Is} = 1 - \frac{\left[\frac{ab}{b+(a-b)(KT/eV)}\right]^3 - \left[\frac{ab}{a-(a-b)(KT/eV)}\right]^3}{(a^3 - b^3)} \quad (7)$$

Where δI is the fraction of current loss due to back diffusion, K is the Boltzmann constant, T is the air temperature, e is the elementary charge, and V is the applied polarizing potential.

And hence the collection efficiency corresponding to back diffusion loss (fd) can be expressed as follows:

$$f_d = 1 - \frac{\delta I}{Is} \quad (8)$$

Results and Discussion

Volume recombination

According to the equation (1), efficiencies considering volume recombination were evaluated for continuous radiation, and the equation (3) was used for estimating collection efficiencies in pulsed radiation.

Continuous radiation

Efficiencies fv values were evaluated for ion chambers under study for continuous radiation and plotted as shown in Figure 1 which represents saturation curves for A3 Exradin ion chamber (Figure 1A), A4 (Figure 1B), A5 (Figure 1C), A6 (Figure 1D), and A8 (Figure 1E) over a wide range of polarizing potential which is not limited to values recommended by the manufacturer.

In Figure 1A, saturation curves for the A3 chamber were evaluated for different $\dot{q}$ values ranging from 9.07×10^{-5} to 3.02×10^{-3} $cm^{-3}s^{-1}$, resulting in a range of volume recombination efficiencies (f_V) starting from 0.70 at the lowest value of polarizing potential (200 V) and high charge rate values (3.02×10^{-3} $cm^{-3}s^{-1}$); its small volume helped in the measurement of high ionization intensity radiation [22]. As the charge rates decrease, efficiency increases. However, it is noticeable that some curves in Figure 1A, 1E cannot reach saturation even at high values of polarizing potential because of the high charge rate values used. This reflects the occurrence of significant volume ion recombination at high charge rates even if very high values of the applied potential were used. Similar curves were obtained for the A4 chamber as shown in Figure 1B, where $\dot{q}$ values are ranging from 4.54×10^{-5} to 7.26×10^{-4} $cm^{-3}s^{-1}$, while the range used for Figure 1C concerning the ion chamber A5 started from 6.35×10^{-7} to 2.99×10^{-4} $cm^{-3}s^{-1}$. For large-volume chambers, A6 and A8, extremely low charge rate values were used: for A6, $\dot{q}$ ranged from 2.99×10^{-8} to 6.35×10^{-7} $cm^{-3}s^{-1}$ while for A8 $\dot{q}$ ranged from 2.99×10^{-8} to 2.99–10^{-7} $cm^{-3}s^{-1}$.

Because of the difference in volume and other dimensional characteristics between A3 (3.6 cm^3) and A4 (30 cm^3) it is noticeable that collection efficiency (f_v) of A4 is lower, for example, at charge rate $\dot{q}=9.07\times10^{-5}$ $cm^{-3}s^{-1}$, and using a polarizing potential of 700 V, f_v for the A3 chamber was 0.9993 while for the A4 chamber it was 0.9877 which means that f_v decreased by a factor of 1.15%, similarly for the A5 chamber (100 cm^3), at the conditions, f_v was 0.9449 i.e. less than for A3 by a factor of 5.4% and less than for A4 by a factor of 4.3%. At a much lower charge rate value ($\dot{q}=9.07\times10^{-7}$ $cm^{-3}s^{-1}$), A6 (800 cm^3) had volume collection efficiency of (f_v)=0.9989 using polarizing potential of 700 V, while 0.8678 for the A8 ion chamber (15700 cm^3). i.e. lower than for A6 by a factor of 13.12%. Figure 2 represents the relation between the volume collection efficiency as a function in the volume of the ion chamber evaluated at different charge rate values ($\dot{q}$) evaluated at polarizing potential of V=700 V. This Figure does not represent a uniform behavior. This is because the chamber volume is not the influencing factor in defining f_v (it is the effective electrode spacing [d]), and however, the general trend in Figure 2 clarifies the

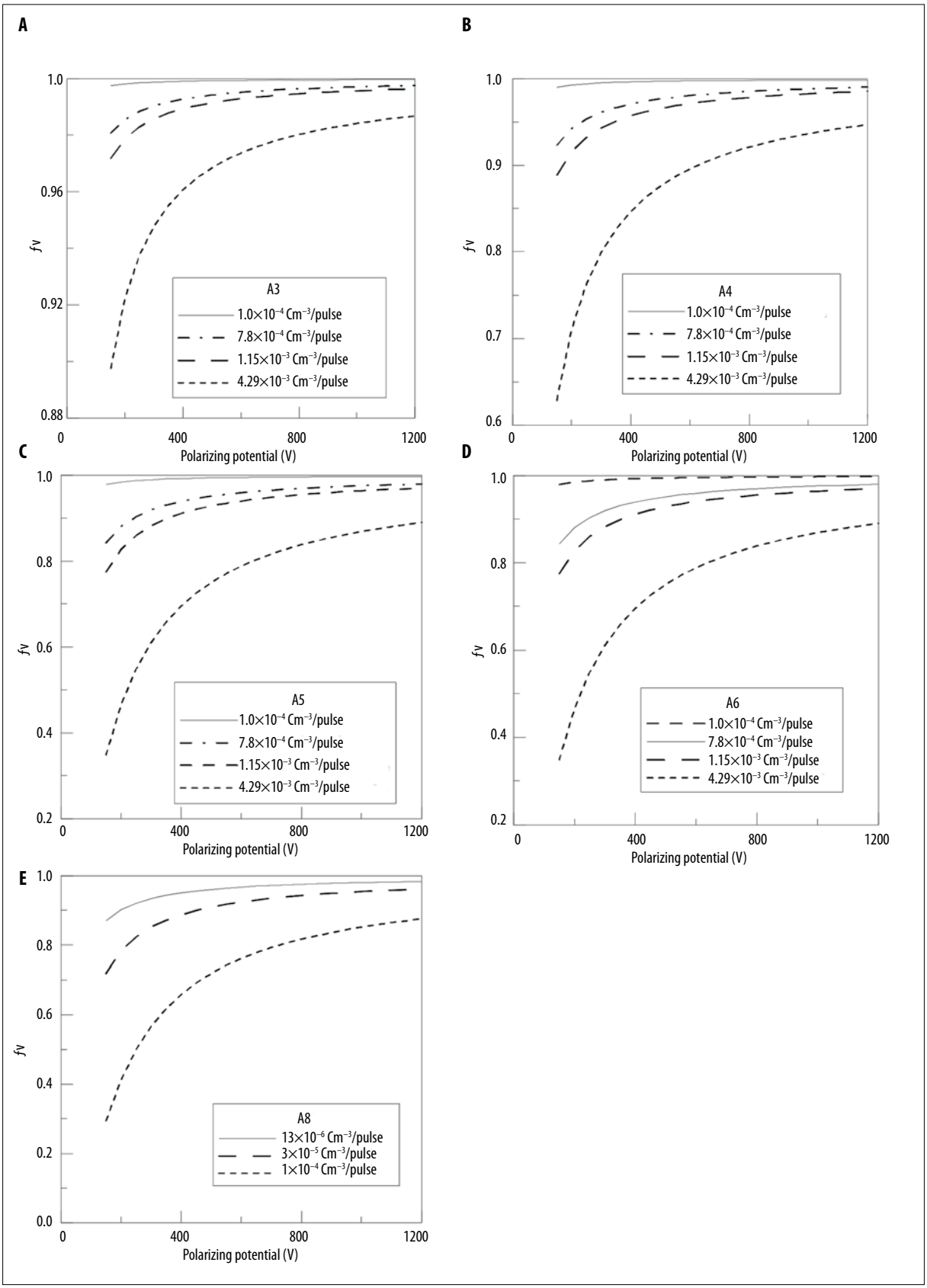

Figure 3. Evaluated collection efficiencies (f_V) in pulsed radiation for different ion chambers as a function in the applied polarizing potential in an ascending order with respect to the chamber volume, values evaluated at different values of charge rate per unit volume ($\dot{q}$): (**A**) A3-Exradin, (**B**) A4-Exradin, (**C**) A5-Exradin, (**D**) A6-Exradin, (**E**) A8-Exradin.

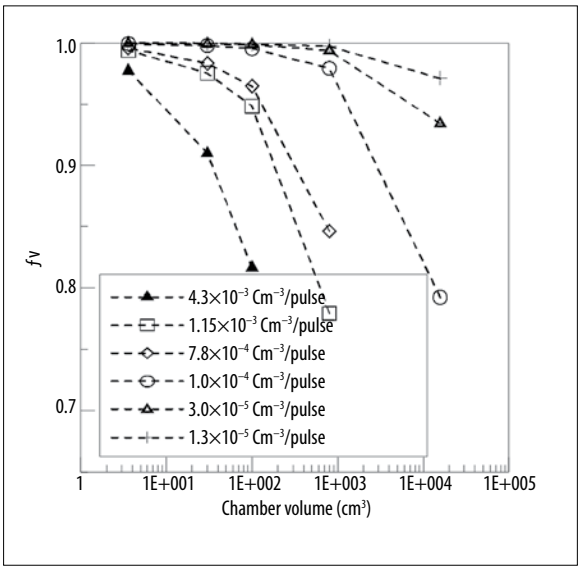

Figure 4. Volume collection efficiency for pulsed radiation (f_V) values corresponding to different values of chamber volume (cm^3) evaluated at different charge density per pulse values (q).

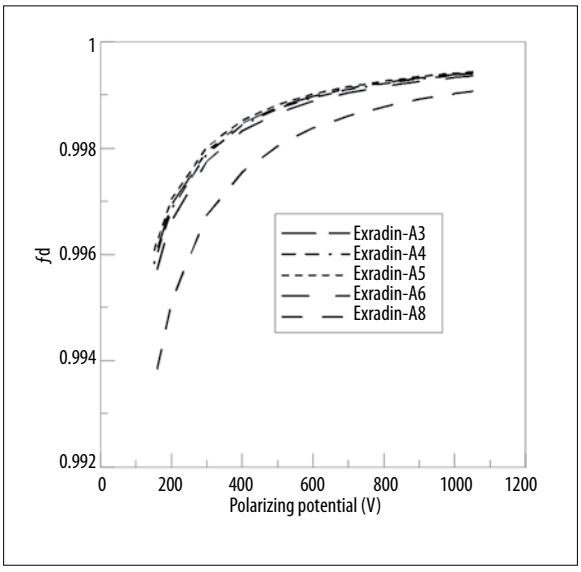

Figure 6. The relation between the change in applied voltage and the calculated collection efficiency considering diffusion current loss (f_d)) for different spherical ion chambers.

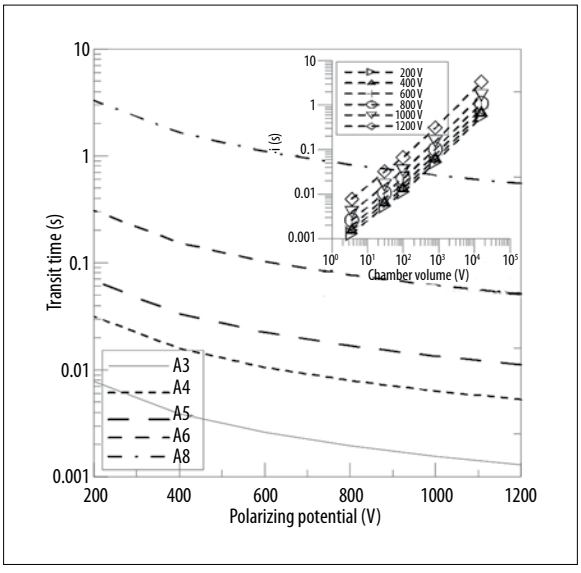

Figure 5. Transit time (τ_i) as a function in applied polarizing potential, inset: the linear relation between τ_i (s) and the chamber volume (cm^3).

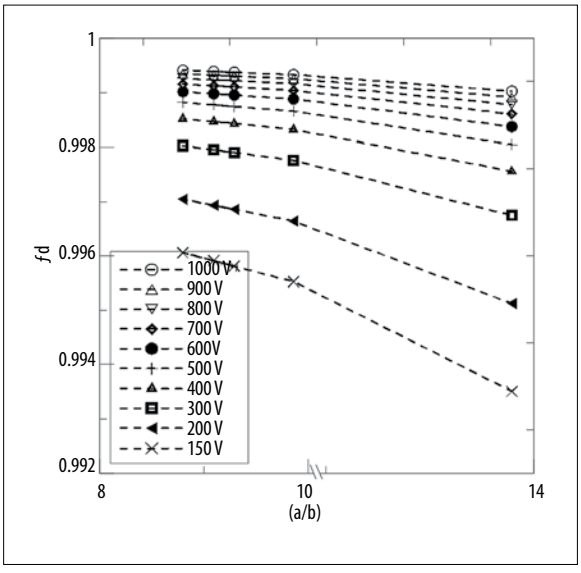

Figure 7. Diffusion current as a function in the ratio (a/b) evaluated at different values of applied polarizing potential in the range (150 V: 1000 V) for spherical ion chambers.

decrease of f_v as the chamber volume increases, this may be due to the special geometrical or technical requirements for the design of large-volume ion chambers. Similar figures like Figure 2 can be plotted for other V values.

Pulsed radiation

Volume collection efficiencies *fv* were evaluated for the five ion chambers under study for pulsed radiation and plotted as shown in Figure 3 which represents saturation curves for the A3 Exradin ion chamber (Figure 3A), A4 (Figure 3B), A5 (Figure 3C), A6 (Figure 3D), and A8 (Figure 3E) over a wide range of polarizing potential (150–1200) V, which is not limited to values recommended by the manufacturer.

As shown in Figure 3A, a wide range of charge density per pulse (*q*) values were used for the evaluation of *fv* where *q* ranged from 1.0×10^{-4} to 4.23×10^{-3} cm^{-3}/pulse. The same range for *q* values was used in Figure 3B–3D, while for Figure 3E a range from 13×10^{-6} to 1.0×10^{-4} cm^{-3}/pulse was used for the evaluation of f_v. Similar to the case of continuous radiation, curves corresponding to high ionization charge density per pulse (q) do not reach saturation even at a very high applied polarizing potential (V); this encounters a significant ion recombination.

Figure 4 represents the relation between the chamber volume (cm^{-3}) and the evaluated collection efficiencies (f_v) over a wide range of charge density per pulse (*q*) values at

polarizing potential of V=700 V. From Figure 4, and despite the absence of a certain behavior regarding the change in *fv* as a function in the chamber volume, it is noticeable that f_v decreases as the chamber volume increases; for example at the same charge density per pulse, $q=7.8\times10^{-4}$ cm^{-3}/pulse which is corresponding to a high ionization intensity, *fv* for the A4 ion chamber is found to be 1.27%, i.e. less than that for the A3 ion chamber and 1.89% higher than that for the A5 ion chamber, while the A6 ion chamber had f_v of about 12.27%. i.e. less than A5 and a very poor value for the A8 ion chamber because of the high *q* value. At a much lower *q* value, $q=1.3\times10^{-5}$ cm^{-3}/pulse, f_v values became better and closer to each other; *fv* for the A4 ion chamber was only 0.02% lower than that for A3, and 0.03% higher than f_v of the A5 ion chamber, while A6 showed f_v value of 0.21% lower than that of A5 and even the A8 ion chamber volume efficiency, f_v was 0.9971 which was 2.88% lower than that of A3.

For large chambers, it was found that recombination effects due to transit-time effects is quite significant [23]. This may be the reason for lower *fv* values for larger chambers compared to the small ones. Transit time (τ_i) for ions in an ionization chamber can be estimated according to the following formula [23]:

$$\tau_i = \frac{d^2}{(Vk_i)} \quad (9)$$

where V is the applied potential, *d* is the effective electrode separation, and *ki* is the mobility of the produced ion and was assumed to be 1.58×10^{-4} m^{2}V^{-1}s^{-1} [24].

Transit time (τ_i) was evaluated for the chambers included in this study and over a range of the applied potential of (200–1200) V and is represented in Figure 5. As shown in that figure, transit time decreased in a power trend as the applied potential (V) increased, and it is clear from the inset of the figure that at constant V, transit time increases as the chamber volume increases. For the chamber A3, τ_i was 0.078 s at 200 V of the applied voltage, and reached 0.0013 s at 1200 V. On the other hand, A8, the largest among the studied ion chambers, had a τ_i value of 1.097 s at 600 V while it decreased to become 0.548 s at V=1200 V. Close values were obtained by Geleijns et al., [23] where transit time (τ_i) was evaluated for the A5 Exradin ion chamber resulting in a value of 0.050 s at an ambient polarizing potential (300 V). The value obtained through this work for the same conditions was 0.045 s. However, dimensions mentioned for the A5 ion chamber are slightly different from those mentioned in this work.

Back diffusion

The collection efficiency corresponding to back diffusion loss (f_d) for different ion chambers was evaluated according to the equation (8). As shown in Figure 6, f_d increased non-linearly as the applied polarizing potential increased; according to the figure, the highest value of f_d was achieved by two ion chambers, A5 followed by A3 and A4, while the lowest values of *fd* were those of A6 and A8, for example, at a value of the applied polarizing potential V=500 V, f_d was 99.88% for A5, and 99.87% for A3 and A4, while for A6 and A8 it was 99.86% and 99.80%, respectively.

Figure 7 represents the relation between the ratio of the inner radius of the outer electrode to the outer radius of the inner electrode (a/b) and the calculated values of f_d. This relation is an inversely linear relation, as it clearly follows from the figure, i.e. as the ratio a/b increases, the values of f_d decrease. The range of (a/b) values was started by 8.8 which corresponded to A5 Exradin, followed by 9.10 for A3, 9.29 for A4, 9.86 for A6 and it ended at the value of 13.89 for A8. A linear relationship was confirmed for different values of the applied polarizing potential ranging from 150 V to 1000 V.

Conclusions

Collection efficiencies considering volume recombination were evaluated for five spherical ion chambers of common types and of different volumes ranging from 3.6 cm^3 to 15700 cm^3, for continuous and pulsed radiation over wide ranges of polarizing potential. The relation between the ion chamber volume and its evaluated collection efficiencies were studied for both continuous and pulsed radiation; transit time for the ion chambers included in this study was evaluated at different values of applied potential. Also, diffusion current values were evaluated for those chambers and hence their collection efficiencies considering diffusion current were calculated and plotted versus the applied polarizing potential and versus the (a/b) ratio. It was found that f_d increases as the applied polarizing potential increases non-linearly and decreases linearly as the (a/b) ratio increases.

References:

1. ICRU: Report 24, International Commission on Radiation Units and Measurements, Bethesda, MD. 1976
2. Andreo P, Suentjens JP, Podgorsan EB: Calibration of Photon and Electron Beams, Radiation Oncology Physics, A Hand book for Teachers and Students, IAEA, Vienna, 2005; 301
3. International Atomic Energy Agency, Absorbed Dose Determination in Photon and Electron Beams, An International Code of Practice, Technical Reports Series No. 277, IAEA, Vienna, 1987
4. International Atomic Energy Agency, Absorbed Dose Determination in External Beam Radiotherapy: An International Code of Practice for Dosimetry based on Standards of Absorbed Dose to Water, Technical Reports Series No. 457, IAEA, Vienna, 2000
5. International Atomic Energy Agency, Dosimetry in Diagnostic Radiology: An International Code of Practice, Technical Reports Series No. 457, IAEA, Vienna, 2007
6. Deutsches Institut für Normung, DIN 6800: Procedures of dosimetry with probe type detectors for photon and electron radiation – Part 2: Ionization chamber dosimetry of high energy photon and electron radiation, 2008
7. Almond PR1, Biggs PJ, Coursey BM et al: AAPM's TG-51 protocol for clinical reference dosimetry of high energy photon and electron beams. Med Phys, 1999; 26(9): 1847–70
8. Khan F: The physics of radiation therapy, 4th ed., Lippincott Williams and Wilkins, 2009
9. Takata N, Tran T, Kim E et al: Loss of ions in cavity ionization chambers. Appl Radiat Isot, 2005; 63: 805–8
10. Maghraby AM: A numerical evaluation of the Boag's collection efficiency formula for some common ion chambers. Isotope and Radiation Research, 2006; 38(2): 319–33

11. Takata N: Ion loss due to initial recombination in a parallel-plate cavity ionization chamber. Phys Med Biol, 1994; 39: 1037–46
12. Takata N: The effects of humidity on volume recombination in ionization chambers. Phys Med Biol, 1994; 39: 1047–52
13. Böhm J: Saturation corrections for plane parallel ionization chambers. Phys Med Biol, 1976; 21: 754–59
14. Attix F: Introduction to Radiological Physics and Radiation Dosimetry. John Wiley & Sons, weinheim, 1986
15. Gryziński MA, Golink N, Zielczyński M: Initial recombination of ions in ionization chambers filled with hydrocarbon gases. Nukleonika, 2007; 52(1): 7–12
16. Begum A, Takata N: Recombination parameters in some fabricated ionization chambers. Bangladesh Journal of Medical Physics, 2011; 4(1): 101–6
17. Boag J: Ionization chambers radiation dosimetry. Vol II, ed F H Attix and W C Roesch (New York: Academic), 1966
18. Boutillon M: Volume recombination parameter in ionization chambers. Phys Med Biol, 1998; 43(8): 2061–72
19. ICRU,. Report 34, International Commission on Radiation Units and Measurements, Bethesda, MD, 1982
20. Havercroft J, Klevenhagen S: Ion recombination corrections for plane-parallel and thimble chambers in electron and photon radiation. Phys Med Biol, 1993; 38: 25–38
21. Takata N, Takeda N, Yin Z: Decrease in output currents due to back diffusion of ions in ionization chambers. Rad Protec Dosi, 1997; 309–12
22. Boag J, Wilson T: The saturation curve at high ionization intensity. British Journal of Applied Physics, 1952; 3: 222–29
23. Geleijns J, Broerse JJ, Zweers D: General ion recombination for ionization chambers used under irradiation conditions relevant for diagnostic radiology. Med Phys, 1995; 22: 17–22
24. Biggs PJ, Nogueira IP: Measurement of the collection efficiency of a large volume spherical ionization chamber in megavoltage therapy beams. Med Phys, 1999; 26: 2107–12